

## Desorption Kinetics of Methanol from Al<sub>2</sub>O<sub>3</sub>(0001) Studied Using Temperature-Programmed Desorption and Isothermal Desorption

S. Y. Nishimura, R. F. Gibbons, and N. J. Tro\*

*Department of Chemistry, Westmont College, 955 La Paz Road, Santa Barbara, California 93108*

*Received: March 25, 1998; In Final Form: June 11, 1998*

Temperature-programmed desorption (TPD) and isothermal desorption were used to investigate the desorption of methanol from Al<sub>2</sub>O<sub>3</sub>(0001) in ultrahigh vacuum. At low coverages, TPD traces for methanol displayed one broad peak that was attributed to monolayer desorption. A second, multilayer peak was observed at a lower temperature as the coverage was increased. The multilayer peak appeared at coverages well below the saturation coverage of the monolayer peak, implying that the multilayer was forming before the monolayer was completely full. Isothermal desorption studies were performed in the multilayer regime as a function of coverage and temperature. The coverage-dependent studies showed that multilayer desorption was of order  $n = 0.53 \pm 0.12$ . The temperature-dependent studies showed that the multilayer activation barrier for desorption was  $11.1 \pm 0.5$  kcal/mol with an  $n = 0.53$  order preexponential of  $3.1 \times 10^{24} \text{ s}^{-1}$ . The approximately half-order desorption from the multilayer is interpreted in terms of a structured multilayer. In the monolayer regime, methanol adsorbs reversibly onto the Al<sub>2</sub>O<sub>3</sub>(0001) surface. The desorption peak is very broad, and quick temperature ramps to temperatures within the monolayer TPD peak show that a distribution of adsorption sites occur on the surface. The TPD traces were modeled assuming first-order desorption kinetics and using a Gaussian distribution of adsorption sites centered at a desorption activation barrier of 17.7 kcal/mol with a width (fwhm) of 3.0 kcal/mol. A first-order preexponential of  $10^{13} \text{ s}^{-1}$  was assumed in the model, and the results were in good agreement with the experimental data. The relatively high desorption activation barrier suggests a strong interaction between the methanol and the surface, most likely due to oxygen lone pair interactions with aluminum. The distribution of adsorption sites suggest that aluminum oxide surfaces, even in single crystals, are very inhomogeneous.

### Introduction

Aluminum oxide surfaces play a significant role in the catalysis of many hydrocarbon reactions.<sup>1–4</sup> Not only do these surfaces act as supports for catalytically active metals but also they often play a direct role in the catalytic process itself.<sup>1,4</sup> The adsorption and desorption of methanol on oxide surfaces is of particular interest since methanol synthesis over oxide-supported catalysts is of great industrial importance. The adsorption, desorption, and surface chemistry of methanol have been examined extensively of single-crystal metal surfaces,<sup>6–16</sup> but few studies exist on single-crystal oxide surfaces.<sup>17</sup> In this study, we utilize TPD and isothermal desorption to examine the desorption of methanol from Al<sub>2</sub>O<sub>3</sub>(0001) in the submonolayer and multilayer regimes.

### Experimental Section

The ultrahigh vacuum (UHV) chamber used in these experiments was pumped by tandem turbomolecular pumps with pumping speeds of 170 and 110 L/s and a titanium sublimation pump. The chamber was equipped with an ion gauge and a UTI model 100C mass spectrometer. Background pressures of  $5 \times 10^{-10}$  Torr were maintained during the course of the investigation with the background gas being predominantly hydrogen.

Single crystals of Al<sub>2</sub>O<sub>3</sub>(0001) with dimensions of 2 cm  $\times$  1.5 cm  $\times$  0.75 mm were purchased from Crystal Systems. A tantalum foil, for resistive heating, was sandwiched between

two Al<sub>2</sub>O<sub>3</sub> crystals using small molybdenum clips. The assembly was then mounted at the bottom of a liquid nitrogen cooled cryostat. A chromel–alumel thermocouple was attached directly to one Al<sub>2</sub>O<sub>3</sub> crystal using a high-temperature, alumina-based, ceramic adhesive. The crystals were then cleaned with acetone and methanol and placed in the ultrahigh vacuum (UHV) chamber. The Al<sub>2</sub>O<sub>3</sub>(0001) surface was cleaned in a vacuum by exposure to an oxygen plasma discharge with the crystal at 373 K. Auger analysis by other groups has demonstrated that this procedure produces consistently clean Al<sub>2</sub>O<sub>3</sub> surfaces.<sup>18</sup> A temperature range from 90 to 1100 K was attainable using liquid nitrogen cooling and resistive heating, and the surface was annealed daily at 1000 K for 1 min.

Methanol was purchased from Aldrich and placed in a small stainless steel cylinder attached directly to a variable leak valve. The samples underwent several cycles of freezing, followed by pumping and thawing in order to remove any volatile impurities. The outlet of the variable leak valve was connected to a stainless steel tube with 1/8 in. i.d., which was directed toward the Al<sub>2</sub>O<sub>3</sub> crystal surface for dosing. The distance between the end of the stainless steel tube and the crystal surface was approximately 1 cm.

Temperature-programmed desorption (TPD) traces were acquired by linearly ramping the temperature of the crystal at a rate of 5 K/s while digitizing the ion current of the mass spectrometer. Isothermal desorption measurements were made by rapidly ramping the crystal temperature at approximately 30 K/s until the desired (set) temperature was reached and then

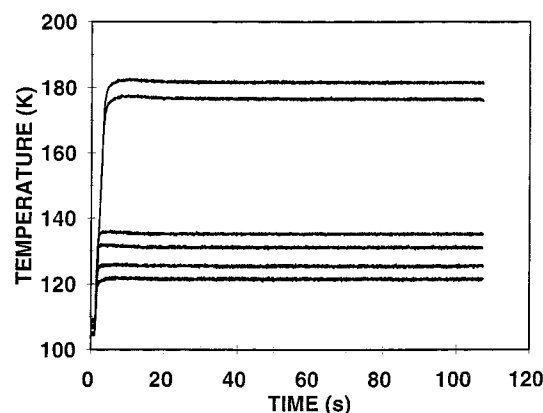


**Figure 1.** Ramp and hold temperature profiles used in isothermal desorption measurements. Temperature overshoot is less than 0.5 K.

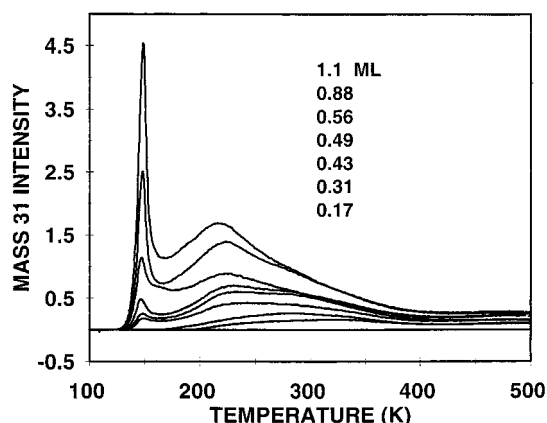


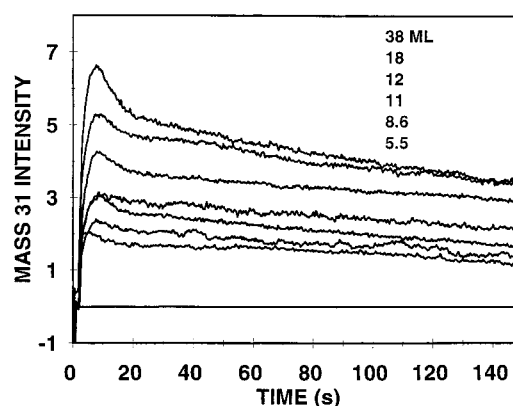
**Figure 2.** TPD traces at a ramp rate of 5 K/s for various methanol coverages on  $\text{Al}_2\text{O}_3(0001)$  at mass 31.

holding the set temperature while digitizing the ion current of the mass spectrometer. A temperature control loop utilizing proportional, integral, and derivative constants (PID) was utilized in both the linear TPD and the ramp and hold experiments. Ramp and hold temperature profiles for several different set temperatures are shown in Figure 1. Temperature overshoot in these experiments was less than 0.5 K, and temperatures could be held constant indefinitely.

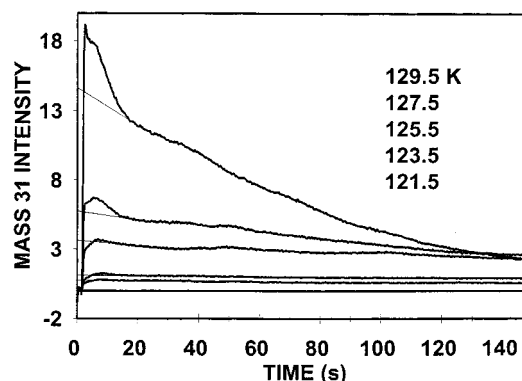
## Results

Figure 2 displays the TPD traces for various methanol coverages on  $\text{Al}_2\text{O}_3(0001)$  at mass 31. Mass 31 is the main peak in the cracking pattern of methanol and is not due to the desorption of methoxy species from the surface. The mass spectrum of desorbing methanol was identical to the mass spectrum observed when methanol was leaked into the chamber, suggesting that methanol desorbs molecularly from  $\text{Al}_2\text{O}_3(0001)$ . At low coverages, the TPD consists of a single, broad peak at approximately 325 K. As the coverage is increased, this peak shifts to lower temperatures and a second, low-temperature peak begins to grow in. The low-temperature peak occurs at about 150 K and is consistent with the desorption of methanol multilayers.<sup>13–15</sup> The multilayer peak, however, begins to grow in before the monolayer (or surface layer) peak saturates. This implies that the multilayer begins to form before the surface layer is completely full.

Figure 3 shows the isothermal desorption traces at 125 K for several coverages of methanol on  $\text{Al}_2\text{O}_3(0001)$ . The peak at the top of each trace is due to the approximately 0.2–0.5 K overshoot in the temperature ramp. Notice that the desorption



**Figure 3.** Isothermal desorption traces at 125 K for several multilayer coverages of methanol on  $\text{Al}_2\text{O}_3(0001)$ .



**Figure 4.** Isothermal desorption traces for approximately 4.4 ML of methanol at various different temperatures.

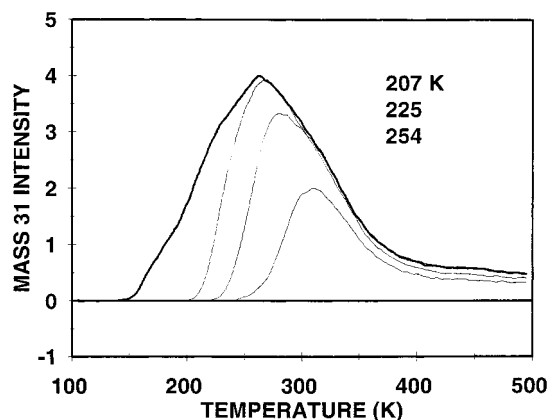
rate, which is proportional to the mass spectrometer intensity in the isothermal desorption trace, is coverage-dependent, even at coverages as high as 38 monolayers (ML). Multilayer desorption rates are often expected to be zero order; however, this is not what we observe for methanol multilayers.

Figure 4 displays isothermal desorption traces for approximately 4.4 ML of methanol at various different temperatures. The total amount of multilayer desorbed for the trace at 125.5 K is approximately 25% of the total coverage. The initial rates of desorption were obtained by extrapolating the linear part of the curve back to zero time. Because the temperature overshoot is slightly greater at higher temperatures, the extrapolations are shown on the graphs.

Figure 5 shows several TPD traces at an initial coverage of approximately 0.20 ML after ramping the surface temperature to several different set temperatures within the monolayer TPD trace line shape. In these experiments, the surface temperature was ramped at 30 K/s to the set temperature and held there for 3 min. The bold TPD trace is a reference TPD in which the temperature was not initially ramped. As the set temperature increases, the low-temperature side of the TPD line shape disappears. As discussed below, this indicates that methanol is desorbing from a range of sites on the  $\text{Al}_2\text{O}_3(0001)$  surface.

## Discussion

The TPD traces shown in Figure 2 show a broad, monolayer (or surface layer) peak and a relatively sharp multilayer peak. The multilayer peak begins to grow in at coverages well below the saturation of the surface layer peak, implying the multilayer begins to grow before the surface is completely covered. The relative areas of the surface layer and multilayer peaks as a function of coverage were simulated with a simple statistical



**Figure 5.** TPD traces at a ramp rate of 5 K/s for an initial coverage of 0.20 ML after ramping the surface temperature to several different set temperatures within the monolayer TPD trace line shape.

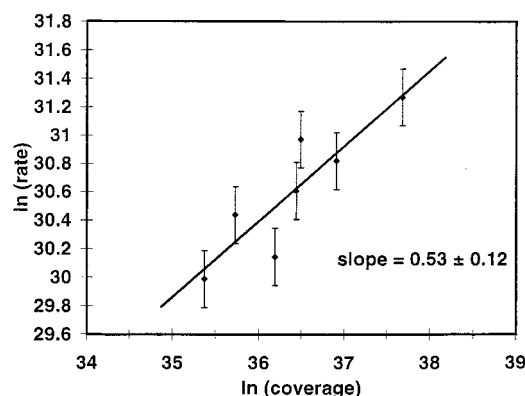


**Figure 6.** Plot of the natural log of initial desorption rate versus the natural log of the coverage for methanol multilayer desorption. The slope indicates that the desorption order is  $n = 0.53 \pm 0.12$ .

sticking model employed previously.<sup>19</sup> Briefly, the model utilized 3000 surface sites and allowed them to be randomly occupied with no surface migration following adsorption. As the sites filled, no preference was given to empty sites over occupied ones; the probability of occupying any one site was the same. By performing the calculation at different total coverages, the relative number of molecules in the surface layer and the multilayer could be calculated. In this simulation the surface layer does not saturate until the equivalent of over 2.5 ML of total coverage is adsorbed. The multilayer begins to fill at coverages as low as 0.1 ML. The results of this model were compared to the experiment by determining the relative areas in the surface layer and multilayer peaks in the experimental TPD traces. The data were scaled with a single parameter, which then determined the reported coverages. The multilayer peaks shown in Figure 2 do not have a common leading edge, implying that the desorption order may not be zero as is often expected for multilayer desorption.

The isothermal multilayer desorption rates shown in Figure 3 were coverage-dependent, even at coverages as high as 38 ML. Figure 6 shows a plot of the natural log of initial desorption rate versus the natural log of the coverage. The initial desorption rates were obtained by extrapolating the linear part of the isothermal desorption curves back to zero time. The coverages were obtained from TPD areas corresponding to an identical dose. The plot has a slope of  $0.53 \pm 0.12$  indicating a desorption order of approximately one-half. We note that these results were the same even if the film was well-annealed near the desorption temperature (120 K for 100 s).

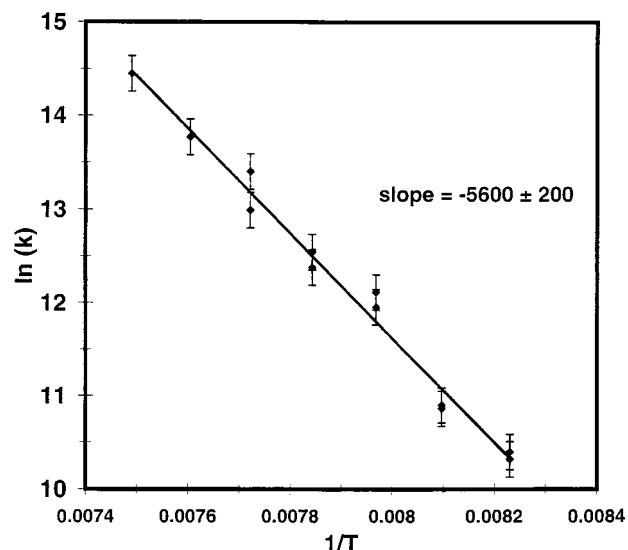


**Figure 7.** Arrhenius plot for the temperature-dependent multilayer desorption rates shown in Figure 5.

Methanol multilayer desorption has been examined by several other groups.<sup>13–15,17</sup> In some studies, zero-order desorption was inferred from TPD traces.<sup>13,15</sup> However, some groups, on the basis of TPD line shapes, have suggested that the desorption order is fractional owing to hydrogen bonding.<sup>14,17</sup> Our coverage-dependent experiments demonstrate that the desorption kinetics are indeed fractional order with an order close to one-half. Multilayers are expected to desorb with zero-order desorption kinetics if the multilayer adsorbs and desorbs in a layer-by-layer fashion; desorption of one layer exposes the next layer, which has an identical number of molecules available to desorb. However, we know from our coverage-dependent TPD experiments that the multilayer does not grow layer-by-layer, but, rather, the multilayer begins to fill before the surface layer is covered. It may be—since methanol forms hydrogen bonds—that the multilayer grows with some kind of microscopic structure. For example, the multilayer may form spherical or cylindrical structures on the surface. As molecules desorb from these structures, their volume decreases and the amount of exposed surface area changes. The surface area of simple geometrical structures such as cones, cylinders, cubes, or spheres will vary with volume raised to the  $2/3$  power. However, if the aspect ratio of these geometric shapes is made extreme, the surface area will be less dependent on changes in volume. In the most extreme case, such as a cube that is extremely wide but very thin, the surface area does not change with volume. Since volume and coverage are directly proportional, our observed desorption order is consistent with a multilayer that forms microscopic structures. Since many different structures give similar surface area to volume dependences, we cannot speculate as to exactly what kind of structure is formed, but we can say that the multilayer does not desorb layer-by-layer, but rather from microscopic structures, such as cylinders, cones, or spheres, whose surface area decreases as desorption occurs.

Figure 7 displays an Arrhenius plot for the temperature-dependent desorption rates shown in Figure 4. A linear regression of the Arrhenius plot revealed that the multilayer activation barrier for desorption was 11.1 (0.5 kcal/mol with an  $n = 0.53$  order preexponential of  $3.1 \times 10^{24} \text{ s}^{-1}$ ). The bulk heat of vaporization for methanol at 150 K is 10.2 kcal/mol,<sup>20</sup> and the bulk heat of fusion at 176 K is 0.52 kcal/mol.<sup>21</sup> Therefore, the bulk heat of sublimation is 10.7 kcal/mol. Our

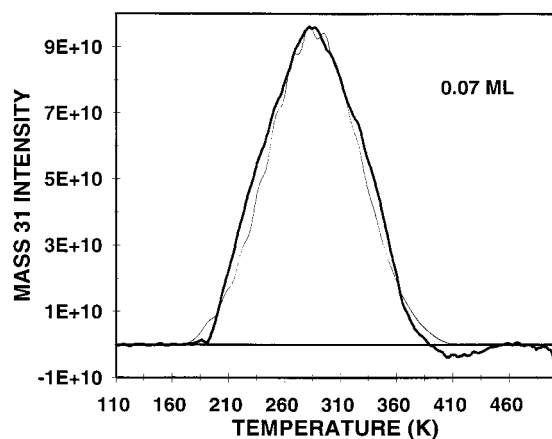


**Figure 8.** Simulation (thin line) of the monolayer TPD trace (bold line) based on a Gaussian distribution of desorption sites on the surface. The best fit was obtained for a center activation barrier of 17.7 kcal/mol and distribution (fwhm) of 3.0 kcal/mol.

multilayer desorption activation barrier of 11.1 kcal is, within our error limits, identical to the bulk heat of sublimation.

In the monolayer regime, the desorption kinetics are quite different. The data shown in Figure 5, in which the temperature of the surface is ramped to a temperature within the TPD line shape before a TPD is taken, are the TPD equivalent of optical hole burning, often used in spectroscopy to determine the homogeneity of a sample. In the optical technique, a narrow band of light is used to photochemically or photophysically burn out a fraction of molecules that absorb those particular wavelengths of light. If the system is inhomogeneously broadened, then an absorption spectrum taken after the hole burning reveals a "hole" in the line shape. If the line is not inhomogeneous, the entire peak intensity decreases. In the TPD equivalent, a temperature ramp to a temperature within the TPD line shape will lead to the loss of the low-temperature side of the peak if the peak is inhomogeneous; reduction of the entire TPD peak without a change in shape indicates a homogeneous peak. The data in Figure 5 show a loss of the low-temperature side of the TPD peak when the crystal temperature is ramped to temperatures within the TPD line shape. Further, the TPD line shape for the "hole-burned" TPD is significantly different than for a normal TPD at the same coverage. The normal TPD traces fit well to a Gaussian line shape, while those for the hole-burned TPD do not. We note also that at these coverages the TPD line shape does not change if the adlayer is annealed near, but below, the desorption temperature. We interpret these data in terms of desorption from a distribution of surface sites. To quantify this distribution, we performed a simple simulation in which we allowed a Gaussian distribution of adsorption sites on the surface. We then modeled what the TPD line shape would look like using first-order desorption kinetics. We assumed a desorption preexponential of  $1 \times 10^{-13} \text{ s}^{-1}$  and varied the center desorption activation barrier, as well as the spread in the distribution of activation barriers, to fit our experimental TPD trace. The results are shown in Figure 8. The best fit for a surface coverage of 0.07 ML was obtained when the desorption activation was centered at 17.7 kcal/mol with a width (fwhm) of 3.0 kcal/mol. The relatively good fit of a Gaussian distribution of adsorption sites—expected for surface inhomogeneity—supports our interpretation of the data. The relatively high activation barrier suggests that methanol interacts strongly with the aluminum oxide surface, most likely through oxygen lone pair interactions with aluminum. The distribution of

desorption activation barriers suggests that aluminum oxide surfaces, even single crystals, are significantly inhomogeneous.

## Conclusions

Temperature-programmed desorption (TPD) and isothermal desorption were used to investigate the desorption of methanol from  $\text{Al}_2\text{O}_3(0001)$  in ultrahigh vacuum. Isothermal desorption studies were performed in the multilayer regime as a function of coverage and temperature. The coverage-dependent studies showed that multilayer desorption was of order  $n = 0.53 \pm 0.12$ . The temperature-dependent studies showed that the multilayer activation barrier for desorption was  $11.1 \pm 0.5 \text{ kcal/mol}$  with an  $n = 0.53$  order preexponential of  $3.1 \times 10^{24} \text{ s}^{-1}$ . The approximately half-order desorption from the multilayer is interpreted in terms of a structured multilayer. In the monolayer regime, methanol adsorbs reversibly onto the  $\text{Al}_2\text{O}_3(0001)$  surface. The TPD traces were modeled assuming first-order desorption kinetics and using a Gaussian distribution of adsorption sites centered at a desorption activation barrier of 17.7 kcal/mol with a width (fwhm) of 3.0 kcal/mol. A first-order preexponential of  $10^{13} \text{ s}^{-1}$  was assumed in the model, and the results were in good agreement with the experimental data. The relatively high desorption activation barrier suggests a strong interaction between the methanol and the surface, most likely due to oxygen lone pair interactions with aluminum. The distribution of adsorption sites suggest that aluminum oxide surfaces, even in single crystals, are very inhomogeneous.

**Acknowledgment.** This research was supported in part by the donors of the Petroleum Research Fund, administered by the American Chemical Society, and by a grant from the National Science Foundation (CHE-9510153). N.J.T. gratefully acknowledges David F. Marten and Allan M. Nishimura for many helpful discussions.

## References and Notes

- (1) Tereshchenko, A. D.; Veselov, V. V. *Khim. Tekhnol.* **1987**, 29, 17.
- (2) McCabe, R. W.; Mitchell, P. S. *J. Catal.* **1987**, 103, 419.
- (3) Yomao, M.; Yasumaro, J.; Hovalia, M.; Hercules, D. M. *J. Phys. Chem.* **1991**, 95, 7037.
- (4) Kakhniashvili, G. N.; Mischenko, Yu. A.; Dulin, D. A.; Isaeva, E. G.; Gelibshrein, A. I. *Kinet. Katal.* **1985**, 26, 134.
- (5) Demuth, J. F.; Ibach, H. *Chem. Phys. Lett.* **1979**, 60, 395.
- (6) Sexton, B. A. *Surf. Sci.* **1979**, 88, 299.
- (7) Bhattacharya, A. K.; Chesters, M. A.; Remble, M. E.; Sheppard, N. *Surf. Sci.* **1988**, 206, L845.
- (8) Baudais, F. L.; Boschke, A. J.; Fedyk, J. D.; Dignam, M. J. *Surf. Sci.* **1980**, 100, 210.
- (9) Bowker, M.; Madix, R. J. *Surf. Sci.* **1980**, 95, 190–206.
- (10) Sexton, B. A. *Surf. Sci.* **1981**, 102, 271–281.
- (11) Demuth, J. E.; Ibach, H. *Chem. Phys. Lett.* **1979**, 60, 395.
- (12) Zang, R.; Gellman, A. J. *J. Phys. Chem.* **1991**, 95, 7433.
- (13) Parameter, J. E.; Jiang, X.; Goodman, D. W. *Surf. Sci.* **1990**, 240, 85.
- (14) Christmann, K.; Demuth, J. E. *J. Chem. Phys.* **1982**, 76, 6308.
- (15) Goodman, D. W.; Jates, J. T., Jr.; Madey, T. E. *Surf. Sci.* **1980**, 93, 135.
- (16) Hubek, J.; de Paola, R. A.; Hoffman, F. M. *J. Chem. Phys.* **1984**, 81, 2818.
- (17) Wu, M. C.; Truong, C. M.; Goodman, D. W. *J. Phys. Chem.* **1993**, 97, 9425.
- (18) Poppa, H.; Moorhead, D.; Heineman, K. *Thin Solid Films* **1985**, 128, 252.
- (19) Slayton, R. M.; Aubuchon, C. M.; Camis, T. L.; Noble, A. R.; Tro, N. J. *J. Phys. Chem.* **1995**, 99, 2151.
- (20) Majer, V.; Svoboda, V. *Enthalpies of Vaporization of Organic Compounds. A Critical Review of Data Compilation*; Blackwell Scientific Publications: Oxford, 1985; p 300.
- (21) Maas, L. J. Walbauer, J. *Am. Chem. Soc.* **1925**, 47, 1.